Verification of PARAGON for LWR design Applications

H.Matsumoto and Y.Tahara
Mitsubishi Heavy Industries, Ltd.,
3-3-1, Minatomirai, Nishi-ku,
Yokohama 220-8401, Japan
matsu@atom.hq.mhi.co.jp ; tahara@atom.hq.mhi.co.jp

M.Ouisloumen
Westinghouse Electric Company
P.O. Box 355
Pittsburgh, PA 15230-0355, USA
ouislom@westinghouse.com

ABSTRACT

A very powerful two-dimensional lattice physics code PARAGON [1] was developed. It is based on the current coupling collision probability (CCCP) method with the discrete angular flux (DAF) model. Many benchmark calculations to validate PARAGON were performed, and it was found that PARAGON could predict reactivity very well under several Vm/Vp, temperature, and poison rod conditions. It was also confirmed that PARAGON could handle very large configurations such as a full core model and a spent fuel pool. Moreover, the power distribution in rods can be accurately predicted using PARAGON code.

1.INTRODUCTION

One of our main objectives of developing PARAGON is to expand the geometrical modeling capability beyond the traditional lattice code applications, such as whole core modeling, two-dimensional Baffle/Reflector modeling etc. To perform rack type calculations such as spent fuel pool (SFP) is another example. To represent SFP model, both square and rectangular cells are needed. However, PHOENIX-P, which is a two-dimensional lattice physics code based on both nodal coupling and S_4 methods, can handle only a square cell modeling except for an assembly half gap. Another objective of PARAGON is the capability of generating power distribution in the fuel rods in routine core design calculations. For that purpose, a new resonance self-shielding method SDDM (Spatially Dependent Dancoff Method) was developed. The SDDM is a generalization of the current PHOENIX-P method and it is based on the idea of Stoker and Weiss [2]. If fuel pellet is not divided into sub-rings, this method is completely consistent with the conventional resonance shielding method employed in PHOENIX-P.
This paper discusses benchmark results to validate both PARAGON and its self-shielding method.

2.RESONACE SHIELDING METHOD

As Stoker and Weiss derived in their method [2], neutron spectrum of sub-divided rings in a fuel rod can be described;

$$\phi_i(E) = \left[\frac{\Sigma_{pf}}{\Sigma_{tf}(E)} \{1 - P_{im}(E)\} + P_{im}(E) \right], \quad (1)$$

where, $P_{im}(E)$ denotes the probability that neutrons born in fuel region i and escaping from the fuel suffer their collisions in the moderator. Other notations are well-known. Next, Stoker and Weiss introduced the following assumption;

$$P_{im}(E) = z(E) P^i_{esc}(E), \quad (2)$$

where, $P_{esc}(E)$ is the fuel escape probability and $z(E)$ is the probability that a neutron having escaped from the fuel lump collides in the moderator. So, the $z(E)$ corresponds to the Dancoff factor.

We propose to modify the Stoker and Weiss method by replacing Eq.(2) with another relation for escape probability of a rod in an assembly including the non-lattice Dancoff effect, following the approach adopted by Stamm'ler [3]. To take account of non-lattice effect in an assembly, P_{IJ} was considered.

$$p_{IJ} = p_{ij} + \frac{R p_{ib} p_{bj}}{1 - R p_{bb}} \quad , \quad (3)$$

where, I and J are the regions in assembly, i and j denote the region in infinite lattice, R is a reflection probability of a cell boundary, p_{ib} denotes the probability of neutrons born in the fuel region i to reach the cell boundary without collisions, p_{bj} is the probability of neutrons entering the cell to suffer their first collision in the fuel region j and p_{bb} is the probability of neutrons entering the cell to traverse the cell uncollided.

From Eq.(3), the following Eq.(4) can be obtained.

$$p_{FF} = p_{ff} + \frac{x(1 - p_{ff})^2}{x(1 - p_{ff}) + C}, \quad (4)$$

where

$$x = \frac{4 V_f \Sigma_f}{S_f}, \quad (5a)$$

$$C = \frac{S_b}{S_f t^2_{fb}} \left(\gamma^0_b + \frac{f(1-g)}{1 - f(1-g)} \right), \quad (5b)$$

S_b is the surface of the cell boundary and S_f is the surface of the fuel lump boundary. γ^0_b is the blackness of the cell when the total cross section of fuel is zero. f is the ratio of the assembly surface to that of all the cell surfaces in the assembly, and g is the first-flight reflection probability across the gap. T_{bf} denotes probability of neutrons entering with a cosine distribution through S_b to reach S_f uncollided.

Eq.(4) can easily be transformed to Eq.(6)

$$\gamma_F = \frac{C \gamma_f}{\gamma_f + C} \quad (6)$$

The blackness of the sub-divided fuel region i is described as following Eq.(7) based on the idea of Stoker and Weiss.

$$\gamma_i = \gamma(\rho_i) - \gamma(\rho_{i-1}) = \left(\gamma^i_{BC} - \gamma^i_{AB} \right) - \left(\gamma^{i-1}_{BC} - \gamma^{i-1}_{AB} \right) \quad (7)$$

where, the AB and BC are the chords as shown in Fig.1. Here, the non-lattice effect can be applied to each blackness included in Eq.(7) in the same way as Eq.(6) for the fuel lump. However the non-lattice effect described by 'C' varies according to the fraction of neutrons entering through fuel surface. The fraction is the probability of neutrons entering fuel with a cosine distribution to be included within OAB (or OBC). The probability corresponds to the relative radius ρ as described in the appendix of Ref.[2]. So, Eq.(7) can be transformed as,

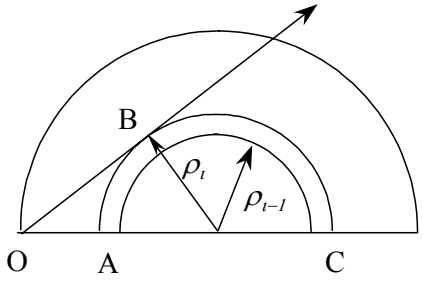

Figure 1. Drawing of a half rod

$$\gamma_I = \frac{\rho_i C \gamma_{BC}^i}{\gamma_{BC}^i + \rho_i C} - \frac{\rho_i C \gamma_{AB}^i}{\gamma_{AB}^i + \rho_i C} - \frac{\rho_{i-1} C \gamma_{BC}^{i-1}}{\gamma_{BC}^{i-1} + \rho_{i-1} C} + \frac{\rho_{i-1} C \gamma_{AB}^{i-1}}{\gamma_{AB}^{i-1} + \rho_{i-1} C} \tag{8}$$

Applying two term rational approximations to Eq.(8) for each term and some well-known relations, the escape probability for a sub-divided ring *I* in an assembly can be obtained.

$$P_{esc}^I = \frac{\gamma_I}{(4V_i / S_f)\Sigma_f} = \sum_{m=1}^{4} F_m \sum_{n=1}^{2} \frac{\alpha_n \beta_n}{\ell_m^i \Sigma_f + \alpha_n} \tag{9}$$

where,

$$\alpha_{1,2} = \frac{(5C+6) \mp \sqrt{C^2 + 36C + 36}}{2(C+1)} \tag{10}$$

$$\beta_1 = \frac{\frac{4C+61}{C+1} - \alpha_1}{\alpha_2 - \alpha_1} \tag{11}$$

$$\beta_2 = 1 - \beta_1 \tag{12}$$

The weighting functions F_m correspond to the ones defined by Stoker as shown in Table I.

ℓ_m^i is a mean chord length of OAB or OBC. It can be generated using Eq.(13).

$$\ell_{\substack{BC \\ AB}}^i = \frac{2R}{\pi}\left(\sqrt{1-\rho_i^2} + \frac{1}{\rho_i}\sin^{-1}\rho_i \pm \frac{\pi}{2}\rho_i\right) \tag{13}$$

Table I. The weighting function of F_m

M	F_m
1	$\frac{S_0 \rho_i \ell_{BC}(\rho_i)}{4V_i}$
2	$-\frac{S_0 \rho_i \ell_{AB}(\rho_i)}{4V_i}$
3	$-\frac{S_0 \rho_{i-1} \ell_{BC}(\rho_{i-1})}{4V_i}$
4	$\frac{S_0 \rho_{i-1} \ell_{BC}(\rho_{i-1})}{4V_i}$

Eq.(9) gives the escape probability that includes the Dancoff effect and it can be used directly for P_{im} in Eq.(1). Therefore, the Eq.(1) yields,

$$\phi_i(E) = \frac{1}{E}\sum_{m=1}^{4} F_m \sum_{n=1}^{2} \frac{\alpha_n \beta_n}{\ell^i_m \Sigma_f + \alpha_n} . \tag{14}$$

The effective resonance cross-section can be described as,

$$\sigma_x(E) = \frac{\int_g \sigma_x(E)\phi(E)dE}{\int_g \phi(E)dE} . \tag{15}$$

Finally substituting Eq.(14) into Eq.(15) yields,

$$\sigma^g_{x,i} = \frac{\sum_{m=1}^{4} F_m \sum_{n=1}^{2} \beta_n I^k_{x,g}(\sigma^{nmk}_{b,j})}{1 - \sum_{m=1}^{4} F_m \sum_{n=1}^{2} \beta_n \frac{I^k_{a,g}(\sigma^{nmk}_{b,j})}{\sigma^{nmk}_{b,j}}} , \tag{16}$$

$$\sigma^{nmk}_b = \frac{\Sigma_b + \alpha_n / \ell^i_m}{N_k} , \tag{17}$$

where Σ_b is the background cross-section of the fuel lump and N denotes number density, and *k, g, a* and *i* denote nuclide, energy-group, absorption, ring-number, respectively.

3.BENCHMARK CALCULATIONS

3.1 REACTIVITY BENCHMARK AGAINST CRITICAL EXPERIMENTS

The well-known critical experiments as "Strawbrige & Barry 101[4]" (101Criticals) used for verification of PHOENIX-P/CP with the 70 group library[5][6] were analyzed again to validate the reactivity prediction of PARAGON. The B&W critical experiments [7], TCA experiments with UO_2 and MOX[8], TCA experiments with B-SUS Plate[9], TCA experiments with gadolinium burnable absorber rods[10] and "KRITZ High Temperature Experiments[11]" were also analyzed.

The B&W critical experiments are selected to validate the modeling of water hole, Pyrex absorber and soluble boron. Validity of the reactivity calculation for change in Vm/Vp, MOX utilization and the boron stainless steel used in the spent fuel pit were checked with TCA cases. The KRITZ apparatus has a pressure tank and is operated up to a maximum temperature of 245 ^oC. The twelve high-temperature critical experiments were analyzed.

Monte-Carlo models, MCNP4B[12], for the experiments except for KRITZ were set up by using Ref.[13] so as to evaluate PARAGON results without the experimental uncertainties. For KRITZ cases, the effective multiplication factors were directly evaluated. The results are shown in Table II to Table VIII.

As shown in Table II, III, IV and V, the reactivity obtained from PARAGON agrees very well with MCNP one. In those cases, the differences between PARAGON and MCNP were within about 0.08%Δk. The results validate PARAGON reactivity calculation.

The reactivity worth measurements of Gd were evaluated with PARAGON as shown in Table VI. The ratios of PARAGON to measurement reactivity worth were less than about 5%.

In KRITZ cases as shown in Table VII, the keff were about 0.47%Δk smaller than measurements. The library used in the analyses was based on ENDF/B-VI mod 3. It has been reported that the library tends to give relatively low reactivity. So, the underestimation seems reasonable. The standard deviation of the ratio between PARAGON and measurements is as small as 0.1%Δk. This means the reactivity calculation method amenable to temperature variations.

Applicability to rack type calculations including B-SUS plate was confirmed comparing to MCNP calculations as shown in Table VIII. The calculational model is shown in Figure 2. It was found that PARAGON agrees well with MCNP considering their standard deviation.

To demonstrate the PARAGON capability for a large-scale model, a typical 3loop PWR core under hot zero power condition (HZP) at the beginning of cycle (BOC) was analyzed. We used 183x183 of both square and rectangular cells, which were fuel cell, control ro guide tube cell, instrumentation thimble cell, assembly half-gap cell, water reflector cell, baffle cell and so on, to model the 3loop core with very high geometrical cell's detail representation. The 70 energy-group and 3 cones of neutron currents were employed in the calculation.
The k-eff of 0.99911 was obtained. The deviation form unity corresponds to the effect of 10 ppm soluble boron concentration. It took 13 hours to terminate the calculation on a 600 MHz ALPHA-21264 processor computer using the executable made with Compaq Fortran 90 full optimization. One can conclude that PARAGON predicts the reactivity very well for a very large and complicated problem.

Table II Comparison of kinf for Strawbrige & Barry101 Criticals

101Critical	(PARAGON-MCNP)/MCNP %
Average	0.06
Standard Deviation	0.19

Statistical Error of MCNP : about 0.0007
Coupling order of PARAGON: 11

Table III Comparison of keff for TCA-UO2 between PARAGON and MCNP4B

Case #	Lattice Name	Lattice Pitch(cm)	Number of Rods in One Side	PARAGON	MCNP	Difference (%)
1			19	0.9923	0.9887	0.37
2	1.50U	1.849	20	0.9929	0.9917	0.12
3			21	0.9937	0.9894	0.44
4			17	0.9914	0.9909	0.06
5			18	0.9920	0.9896	0.24
6	1.83U	1.956	19	0.9935	0.9901	0.34
7			20	0.9935	0.9922	0.13
8			21	0.9940	0.9921	0.19
9			16	0.9907	0.9926	-0.19
10			17	0.9916	0.9913	0.04
11	2.48U	2.150	18	0.9924	0.9923	0.01
12			19	0.9925	0.9915	0.10
13			20	0.9925	0.9917	0.08
14			15	0.9903	0.9946	-0.42
15			16	0.9913	0.9933	-0.20
16	3.00U	2.293	17	0.9923	0.9932	-0.09
17			18	0.9927	0.9909	0.17
18			19	0.9930	0.9930	0.00
Average				0.9924	0.9916	0.08
Standard Deviation				0.0010	0.0015	0.21

Statistical Error of MCNP : about 0.0007
Coupling order of PARAGON: 23

Table IV Comparison of keff for TCA-MOX between PARAGON and MCNP4B

Case#	Lattice Name	Lattice Pitch(cm)	Number of Rods in One Side	PARAGON	MCNP	Difference (%)
1				0.9880	0.9888	-0.08
2	2.42Pu	1.825	23	0.9891	0.9897	-0.06
3				0.9896	0.9905	-0.10
4				0.9891	0.9844	0.48
5	2.98Pu	1.956	21	0.9895	0.9812	0.85
6				0.9905	0.9877	0.29
7				0.9897	0.9945	-0.48
8	4.24Pu	2.225	20	0.9904	0.9883	0.21
9				0.9910	0.9869	0.42
10	5.55Pu	2.474	21	0.9912	0.9946	-0.35
11				0.9913	0.9951	-0.38
Average				0.9899	0.9892	0.07
Standard Deviation				0.0010	0.0044	0.41

Statistical Error of MCNP : about 0.0007
Coupling order of PARAGON: 23

Table V Comparison of kinf for B&W between PARAGON and MCNP4B

Loading	Fuel Rods	Water Holes	Pyrex Rods	Soluble Borron(ppm)	PARAGON	MCNP	Difference (%)
1	4961	0	0	1511	1.0144	1.0142	0.02
2	4808	153	0	1334	1.0128	1.0127	0.01
3	4808	153	0	1337	1.0157	1.0135	0.22
4	4808	117	36	1183	1.0160	1.0130	0.29
5	4808	117	36	1181	1.0138	1.0127	0.11
6	4808	81	72	1034	1.0134	1.0139	-0.05
7	4808	81	72	1031	1.0128	1.0123	0.05
8	4808	9	144	794	1.0113	1.0122	-0.09
9	4808	9	144	779	1.0117	1.0117	0.00
Average					1.0135	1.0129	0.06
Standard Deviation					0.0016	0.0008	0.12

Statistical Error of MCNP : about 0.0007
Coupling order of PARAGON: 11

Table VI Comparison of Gd reactivity worth in TCA between PARAGON and measurements

Core Name	Gd Fuel Gd wt%	Gd Fuel Number	PARAGON (%)	Measured (%)	Ratio (PRGN/MEASERD)
S-A	0.00	1	----	----	----
S-B	0.25	1	0.557	0.587	0.949
S-D	1.50	1	0.755	0.779	0.969
S-E	3.00	1	0.814	0.841	0.968
D-a-D	1.50	2	1.401	1.433	0.978
D-b-D	1.50	2	1.448	1.455	0.995
D-e-D	1.50	2	1.338	1.319	1.014
T-a-D	1.50	3	1.863	1.862	1.001

Coupling order of PARAGON: 11

Table VII KRITZ Results obtained with PARAGON

Case	Lattice	Boron (ppm)	Temp (^{o}C)	K-eff
1	39x39	0.8	41.2	0.9965
2	39x39	0.8	90.0	0.9955
3	39x39	0.8	216.6	0.9951
4	39x39	0.8	225.6	0.9953
5	46x46	46.3	90.4	0.9970
6	46x46	46.3	206.0	0.9954
7	46x46	46.3	227.3	0.9960
8	46x46	46.3	245.8	0.9957
9	46x46	175.0	22.4	0.9928
10	46x46	175.0	89.1	0.9955
11	46x46	175.0	201.3	0.9946
12	46x46	175.05	205.3	0.9940
Average				0.9953
Standard Deviation				0.0011

Coupling order of PARAGON: 23

Table VIII Comparison of k-eff in TCA B-SUS cases between PARAGON and MCNP4B

B-10 wt% in B-SUS	B-SUS Thickness(mm)	Water Gap(mm)	Critical Water Height(cm)	PARAGON	MCNP	PRGN/MCNP
0.00	6.0	0.000	82.62	0.9882	0.9869	1.0012
		1.956	86.37	0.9943	0.9933	1.0010
		3.912	82.99	0.9944	0.9923	1.0022
0.67	6.0	0.000	111.12	0.9901	0.9932	0.9969
		1.956	92.21	0.9919	0.9924	0.9994
		3.921	84.74	0.9929	0.9920	1.0009
0.98	3.0	0.000	111.42	0.9900	0.9936	0.9964
	6.0	0.000	113.54	0.9898	0.9929	0.9969
		0.978	104.73	0.9925	0.9952	0.9974
		1.956	95.51	0.9929	0.9942	0.9988
		2.934	90.62	0.9938	0.9942	0.9995
		3.912	87.67	0.9945	0.9940	1.0004
	9.0	0.000	112.55	0.9896	0.9929	0.9967
	12.0	0.000	111.76	0.9898	0.9935	0.9962
Average				0.9918	0.9929	0.9988
Standard Deviation				0.0021	0.0019	0.0021

Statistical Error of MCNP : about 0.0004
Coupling order of PARAGON: 11

3.2 VALIDATION TEST OF POWER DISTRIBUTION

To validate the flux calculation module of PARAGON, the power distribution obtained with PARAGON in the TCA 1.83U 21X21 was compared to MCNP. It is shown in Figure 3. The MCNP calculation was done with 10^{8} histories not to consider the statistical error. From the Figure 3, it is seen that the differences were less than 1% except for near the corner

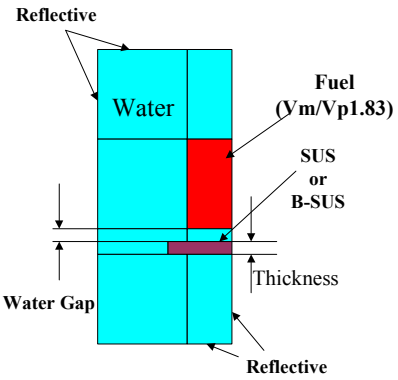

Figure 2 TCA B-SUS Model

pins of the core. Even in the corner area, the error is 2.3% at maximum. This validates the neutron flux obtained with PARAGON.

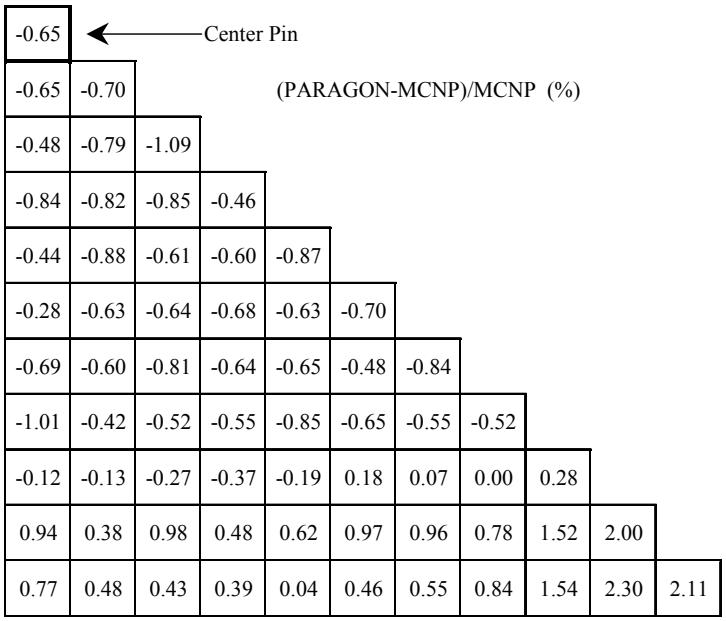

Figure 3 Comparison of power distribution for TCA 1.83U 21X21 core

3.3 VALIDATION TEST OF NEW RESONANCE SHIELDING MODULE SDDM

To validate new resonance shielding method of the SDDM (Spatially Dependent Dancoff Method), the absorption reaction-rates in a depleted UO_2 pellet with 60GWd/t burnup were compared with those obtained from a continuous energy Monte-Carlo code MVP [14]. The specifications of the calculational model is shown in Table IX. The rod used in the calculation was first divided into 10 equal volume rings. Then the outermost ring was divided into 8 equal volume rings. So, the rod was totally sub-divided into 17 rings. The number densities used in the comparison were generated using the depletion calculation of PARAGON. As shown in Table X, the number densities had spatial dependencies. The number densities were put in both codes to represent a depleted rod. The comparison of absorption rates is shown in Figure 4. The relative differences of absorption rate of each isotope and k-inf are shown in Table XI. The k-inf difference between PARAGON and MVP was only 0.06%Δk. The relative difference of absorption-rates were less than about 3% except for Pu-242. Regarding Pu-242, its absolute value is very small, so the large error 15% was observed.

Table IX Specification of the test model for depletion calculation

Cell pitch	1.265 cm
Fuel	UO_2
Radius	0.412 cm
Enrichment(BOL)	4.1wt%U-235
Temperature	900 K
Burnup(Average)	60 GWd/t
Cladding	Zr-4
Outer Radius	0.476 cm
Thickness	0.064 cm
Temperature	600 K
Moderator	H_2O
Temperature	600 K
Boron concentration	500 ppm

The destructive measurements [15] published by CRIEPI were tracked for SDDM validation. The comparison of burnup distribution is shown in Figure 5 with measurements. The pellet was divided

into 17 concentric cylinders in the same manner as in the above MVP comparison case. Very good agreement can be seen.

Table X Number densities in a depleted UO_2 pellet (60GWd/t) generated using PARAGON (10^{24} atom/cm3)

(r/R)	U-235	U-238	Pu-239	Pu-240	Pu-241	Pu-242	Am-241
0.316	1.01E-04	2.07E-02	1.06E-04	6.45E-05	3.37E-05	2.11E-05	1.20E-06
0.447	9.89E-05	2.07E-02	1.07E-04	6.38E-05	3.44E-05	2.18E-05	1.22E-06
0.548	9.71E-05	2.07E-02	1.06E-04	6.23E-05	3.47E-05	2.22E-05	1.23E-06
0.632	9.53E-05	2.07E-02	1.06E-04	6.05E-05	3.49E-05	2.26E-05	1.23E-06
0.707	9.34E-05	2.07E-02	1.08E-04	6.03E-05	3.61E-05	2.35E-05	1.26E-06
0.775	9.14E-05	2.06E-02	1.14E-04	6.18E-05	3.86E-05	2.56E-05	1.34E-06
0.837	8.93E-05	2.06E-02	1.16E-04	6.09E-05	3.97E-05	2.67E-05	1.38E-06
0.894	8.71E-05	2.06E-02	1.24E-04	6.30E-05	4.31E-05	2.94E-05	1.49E-06
0.949	8.46E-05	2.04E-02	1.41E-04	6.83E-05	4.97E-05	3.46E-05	1.71E-06
0.955	8.31E-05	2.02E-02	1.63E-04	7.66E-05	5.79E-05	4.06E-05	1.99E-06
0.962	8.28E-05	2.02E-02	1.72E-04	8.07E-05	6.18E-05	4.37E-05	2.12E-06
0.968	8.24E-05	2.01E-02	1.83E-04	8.50E-05	6.59E-05	4.68E-05	2.26E-06
0.975	8.20E-05	2.00E-02	1.97E-04	9.05E-05	7.11E-05	5.07E-05	2.44E-06
0.981	8.15E-05	1.98E-02	2.15E-04	9.78E-05	7.81E-05	5.61E-05	2.68E-06
0.987	8.10E-05	1.96E-02	2.41E-04	1.08E-04	8.80E-05	6.36E-05	3.03E-06
0.994	8.05E-05	1.93E-02	2.78E-04	1.22E-04	1.02E-04	7.47E-05	3.52E-06
1.000	8.00E-05	1.87E-02	3.51E-04	1.51E-04	1.32E-04	9.78E-05	4.56E-06

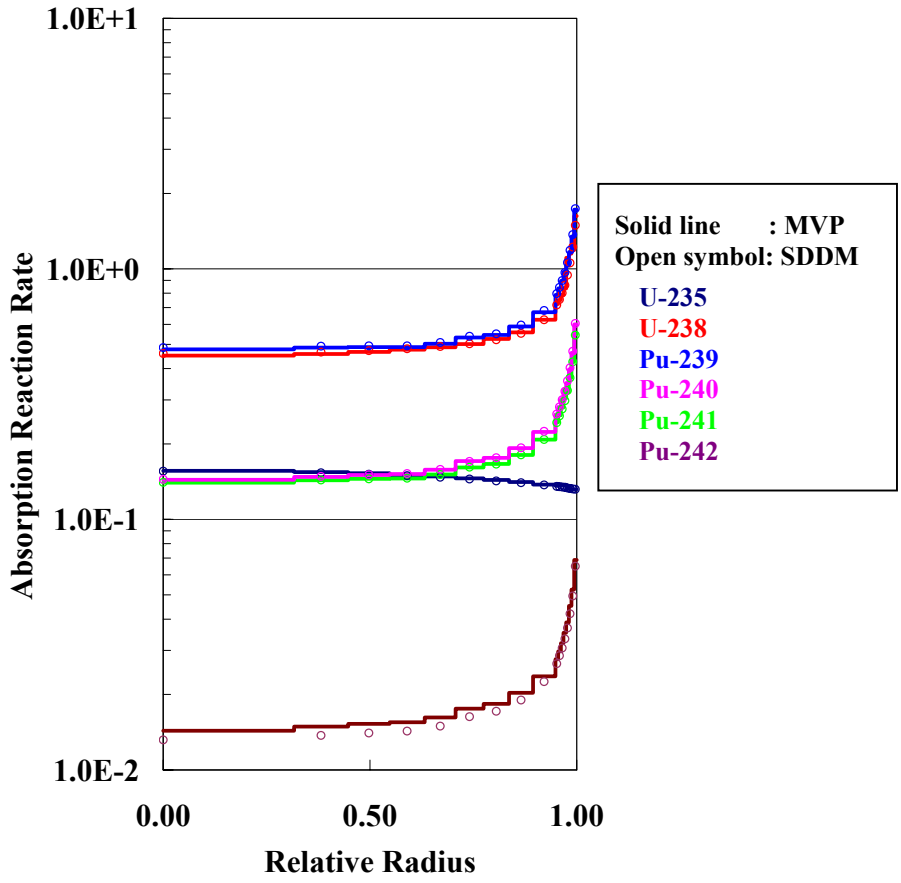

Figure 4 Comparison of absorption Reaction Rates in a depleted UO_2 pellet between SDDM and MCNP

Table XI Comparison of k-inf and absorption reaction rates of a depleted UO2 pellet (60GWd/t)

	K-inf	
PARAGON	1.04448	
MVP	1.04508	(1σ:0.00019)

(Absorption Rate)

(r/R)	U-235	U-238	Pu-239	Pu-240	Pu-241	Pu-242
0.316	3.1	2.1	-2.4	1.3	1.4	-1.8
0.447	3.2	1.6	-2.4	1.2	1.5	-2.4
0.548	3.2	0.9	-2.4	1.0	1.5	-2.4
0.632	3.2	0.1	-2.4	1.0	1.5	-2.6
0.707	3.2	-0.2	-2.5	0.8	1.4	-2.8
0.775	3.2	2.1	-2.5	0.5	1.4	-3.3
0.837	3.3	0.2	-2.5	0.4	1.4	-3.8
0.894	3.2	1.2	-2.5	0.0	1.4	-4.6
0.949	3.2	-0.1	-2.7	-0.1	1.3	-5.9
0.955	3.2	0.9	-2.7	0.0	1.2	-7.2
0.962	3.2	1.0	-2.8	-0.2	1.2	-8.0
0.968	3.1	0.6	-2.9	-0.3	1.1	-8.7
0.975	3.1	0.1	-2.8	-0.4	1.1	-9.5
0.981	3.1	-0.8	-2.9	-0.5	1.1	-10.5
0.987	3.2	-1.6	-2.9	-0.5	1.1	-11.9
0.994	3.1	-2.9	-3.0	-0.8	1.0	-13.4
1.000	3.0	-4.5	-3.2	-1.0	0.8	-15.6

(PARAGON-MVP)/MVP (%)

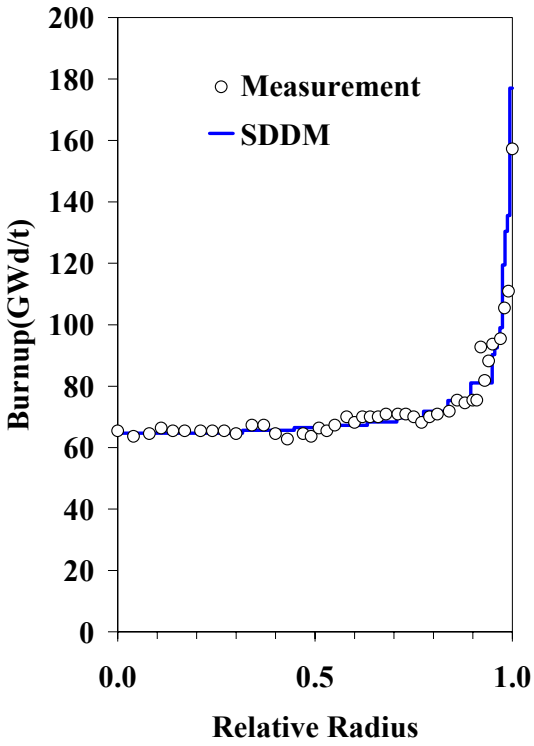

Figure 5 Comparison of burnup distribution in a depleted UO_2 pellet

Conclusion

A very powerful lattice code PARAGON was developed. PARAGON has not only the capability of generating the nuclear constants for a 3D nodal code, but also the capability of generating the power profile within the fuel pellet which is needed in fuel integrity evaluation, as well as the capability of handling very large configurations such as core calculations and spent fuel pit calculations.

Acknowledgments

The authors would like to thank Dr.Y.A.Chao for helpful suggestions and valuable advice.

REFFERENCES

1 M.Ouisloumen, H.C.Huria and H.Matsumoto, ANS International Meeting on Mathematical Methods for Nuclear Applications, Sept.2001, Salt Lake City, Utah, USA

2 C.C.Stoker, J.Z.Weiss, "SPATIALLY DEPENDENT RESONANCE CROSS SECTIONS IN A FUEL ROD," *annals of NUCLEAR ENERGY*, **vol.23, No.9**, pp765-778(1996)

3 R.J.J.Samm'ler, M.J.Abbate, *Method of Steady-State Reactor Physics in Nuclear Design*, Academic Press, London, (1983)

4 L.E.Strawbrige, R.F.Barry, "Critical Calculations for Uniform Water-moderated lattices," *Nucl. Sci. Eng*., **23**, 58(1965)

5 H.C.Huria, Y.Tahara, "New Multigroup Library for PHOENIX-P," PHYSOR96(1996)

6 Y.Tahara, H.Matsumoto, H.C.Huria, M.Ouisloumen, "Critical Experiments Analyses by Using 70 Energy Group Library Based on ENDF/B-VI," *Proc. 1997 Symposium on Nuclear Data*, JAERI-Conf 98-003

7 M.N.Baldwin, M.E.Sten, "Physics Verification Program Part III, Task 4 Summary Report," BAW-3647-20, March 1971

8 H.Tsuruta, et al., "Critical Size of Light-Water Moderated UO_2 and PuO_2-UO_2 Lattices," JAERI1254(1978)

9 Y.Miyoshi, et al., "Reactivity Effect of Borated Stainless Steel Plate in Single and Coupled Cores Composed of Low-Enriched UO2 Rods," *J.Nucl. Sci. Technol*., **31[4]**, pp.335-348(1994)

10 S.Matsuura, et al., "Physical characteristics of Gd2O3-UO2 fuel in LWR," JAERI-M 9844(1981)

11 R.Persson et al., "High-temperature critical experiments with H2O-moderated fuel assemblies in KRITZ," NUCLEX72(1972)

12 J.F.Briesmeister, "MCNP –A general Monte Carlo N-particle transport code, version 4B," LA-12625-M (1997).

13 D.Y.Chung, et al., "*INTERNATIONAL HANDBOOK OF EVALUATIED CRITICALITY SAFETY BENCHMARK EXPERIMENTS*," OECD NEA NUCLEAR SCIENCE COMMITTEE, NEA/NSC/DOC(95), September (1999)

14 T.Mori, et al., MVP/GMVP: General purpose Monte Carlo codes for neutron and photon transport calculations based on continuous energy and multigroup methods, JAERI-Data/Code 94-007(1994)

15 A.Sasahara, et al., "Post irradiation examination and the validity of computational analysis for high burnup UO_2 and MOX spent fuels," Komae Research Laboratory Rep. No. T95012(1996)